ACCOUNTS
of chemical research

Structural Effects in Molecular Metal Halides

MAGDOLNA HARGITTAI

Materials Structure and Modeling Research Group of the Hungarian Academy of Sciences, Budapest University of Technology and Economics, P.O. Box 91, H-1521 Budapest, Hungary

RECEIVED ON SEPTEMBER 19, 2008

CONSPECTUS

Metal halides are a relatively large class of inorganic compounds that participate in many industrial processes, from halogen metallurgy to the production of semiconductors. Because most metal halides are ionic crystals at ambient conditions, the term "molecular metal halides" usually refers to vapor-phase species. These gas-phase molecules have a special place in basic research because they exhibit the widest range of chemical bonding from the purely ionic to mostly covalent bonding through to weakly interacting systems. Although our focus is basic research, knowledge of the structural and thermodynamic properties of gas-phase metal halides is also important in industrial processes. In this Account, we review our most recent work on metal halide molecular structures. Our studies are based on electron diffraction and vibrational spectroscopy, and increasingly, we have augmented our experimental work with quantum chemical computations. Using both experimental and computational techniques has enabled us to determine intriguing structural effects with better accuracy than using either technique alone.

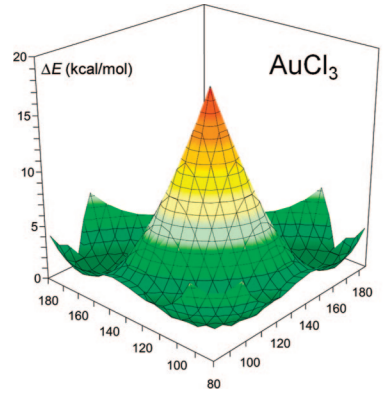

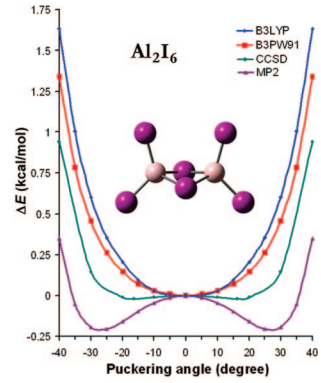

We loosely group our discussion based on structural effects including "floppiness", relativistic effects, vibronic interactions, and finally, undiscovered molecules with computational thermodynamic stability. Floppiness, or serious "nonrigidity", is a typical characteristic of metal halides and makes their study challenging for both experimentalists and theoreticians. Relativistic effects are mostly responsible for the unique structure of gold and mercury halides. These molecules have shorter-than-expected bonds and often have unusual geometrical configurations. The gold monohalide and mercury dihalide dimers and the molecular-type crystal structure of $HgCl_2$ are examples. We also examined spin–orbit coupling and the possible effect of the 4f electrons on the structure of lanthanide trihalides. Unexpectedly, we found that the geometry of their dimers depends on the f electron configuration. Metal halides are unique in exhibiting strong vibronic interactions such as the Jahn–Teller effect and the related Renner–Teller effect. Some metal trihalide molecules have an almost T-shape due to static Jahn–Teller distortions. The nonlinear structure with a 150° bond angle of the chromium dichloride molecule demonstrates the Renner–Teller effect. Finally, we present a few examples of unknown structures that appear to be thermodynamically stable, including gold and silver triiodides and all silver subhalides.

The combination of experimental and computational techniques has brought new insights to the structural chemistry of metal halides. We expect that the continuing progress in computational chemistry will shed further light on the intricate details of these and other molecular structures.

1. Introduction

"Molecular metal halides" usually refers to the vapor phase since most metal halides are ionic crystals at ambient conditions. Vapor-phase metal halides are of interest for both academic and industrial purposes. Their molecules represent the widest range of bonding types and display considerable variations in their properties. They are also important participants in many industrial

Published on the Web 01/26/2009 www.pubs.acs.org
10.1021/ar800205r CCC: $71.50

processes—either by design or as an unwanted side-product, e.g., in chemical vapor transports, metal halide discharge lamps, and combustion processes.

What started in our laboratory as a high-temperature electron diffraction (ED) study of metal halides about 30 years ago has gradually evolved into a more complex program, including quadrupole mass spectrometry, vibrational spectroscopy, and, increasingly, quantum chemical calculations. Our earlier work, together with the complete literature concerning metal halide molecular structures, has been reviewed.[1−3] In this Account, our most important results of the past decade are summarized.[4−23]

Metal halides usually evaporate at high temperatures; hence their experiments require special conditions. Their computational requirements are also different from the mainstream applications of quantum chemistry. This is why the applied methodologies are summarized here. As is demonstrated throughout this Account, the combined use of experiments and computations is superior to using individual techniques separately, but this approach yields reliable results *only* if the data from different techniques are brought to a common denominator.

The computed geometry is the equilibrium geometry corresponding to the minimum of the potential energy surface, whereas ED provides a thermal-average geometry.[3,24,25] Neither the bond lengths nor the molecular shape from computations are exactly the same as those from experiment due to their different physical meanings. A thermal-average bond length might be about 0.02−0.03 Å larger than the equilibrium bond length. The symmetry of the ED structure is usually lower than that of the equilibrium structure; a linear metal dihalide molecule, for example, appears to be bent from ED with an angle of around 160° depending on the temperature of the experiment and on the bending mode of the molecule. As a reference point, the equilibrium geometry is the best. Therefore, for a correct comparison of computed and experimental geometrical parameters, vibrational corrections are applied to the experimental parameters to better approximate the equilibrium geometry.

2. Methodologies

2.1. Electron Diffraction. The vapors of metal halides often contain different oligomers. The vapor composition must be known for their reliable structure determination. Small amounts of contaminants may not be easy to recognize, but they can falsify the structural information on the principal component of the vapor. We found that the use of a quadrupole mass spectrometer, attached to the ED equipment, greatly facilitated the identification and optimization of the vapor composition.

ED is practically the only experimental technique to determine the bond lengths of gas-phase metal halides,[3] usually with high precision. At the same time, due to the thermal-average nature of the ED geometry, the unambiguous determination of molecular symmetry necessitates additional information about the shape of the molecule.

2.2. Quantum Chemical Calculations. A recent volume of *Faraday Discussions* was dedicated to quantum inorganic chemistry,[26] presenting most of the unique characteristics of these computations. Here, we single out a few aspects of our computations; details are given in the original publications. We have found it essential to check different method/basis-set combinations to select the optimal approach for each molecule. Reliable bond lengths from ED are instrumental in this respect, and this is one of the reasons for the success of joint use of ED and computations. We have applied both density functional (DFT) and wave function-based correlated methods and, for most metals, different quasirelativistic or fully relativistic effective core potentials (ECP) and associated basis sets, often augmented with diffuse functions. For transition metal halides, the use of multireference calculations, such as CASSCF, has proved essential to correctly determine the ground electronic state of the molecule. The same was true for lanthanide halides if small-core ECPs were used. Spin−orbit (SO) effects were also considered in selected cases.

Experience shows that the computed bond lengths strongly depend on the method/basis set combinations, and sometimes very large basis sets are needed to get convergence in the bond length, on the one hand, and an agreement with the equilibrium bond length estimated from experiment, on the other. For example, in case of $SrCl_2$, a relatively simple triatomic molecule, we could not reach convergence in the bond length with the correlated calculations even with very large basis sets.[18] Interestingly, the B3PW91 DFT calculations converged quickly, and the result, 2.606 Å, coincided with the equilibrium bond length estimated from electron diffraction, 2.607(13) Å (the numerical coincidence may be spurious, but the agreement is comforting).

The bond angles are usually less sensitive to the choice in computational approach, and this is advantageous when constraints have to be applied in the ED analysis; the bond angles, even from relatively low-level computations, may be assumed in the initial stages of the analysis.

For thermodynamic calculations, the accuracy of vibrational frequencies is an important consideration. Computations tend

to overestimate frequencies, except for low deformation modes of floppy molecules that are generally unreliable due to the very flat potential energy surfaces (PES). Gas-phase infrared spectra are hard to interpret due to the highly populated excited vibrational and rotational levels. The experimental frequencies determined by matrix isolation (MI) spectroscopy usually suffer from matrix effects, sometimes causing only a shift in the frequencies toward smaller values, while in other cases interpretational difficulties occur due to complex formation in the matrix and to changes of molecular symmetry.

2.3. Joint Use of Different Techniques. Concerted use of different techniques greatly enhances structural information not only because they provide more data but also because they beneficially complement each other. Vibrational frequencies from experiment may give information about the molecular symmetry. The most useful information for ED comes from quantum chemical calculations. It can be differences of bond lengths when closely spaced distances cannot be resolved. Using differences of bond lengths rather than their actual values alleviates the problem of difference in the physical meaning of the parameters. Computations are also helpful in other ways; they provide parameters of bending and puckering potentials, vibrational frequencies, or thermodynamic quantities.

The following discussion loosely groups the different structures according to some features without strict dividing lines between them.

3. Floppy Molecules

3.1. Linear versus Bent. As has been described,[3,27] some alkaline-earth dihalides are linear, others are bent, and some are "in between"—we call them quasilinear. The bent structures are favored by core-polarization interactions between the metal and the halogen and by the availability of metal d-orbitals for hybridization with the valence s orbitals.

A quasilinear molecule has a flat bending potential with a barrier at linearity lower than or comparable to its zero-point energy of bending. In our joint ED and computational study of $SrCl_2$, the computational results strongly depended on the method/basis set combination (vide supra).[18] Both DFT and correlated calculations found the molecule to be bent; its strongly anharmonic MP2 bending potential is shown in Figure 1, with a barrier to linearity less than 0.1 kcal/mol. DFT calculations give a three-times-larger barrier, but considering the uncertainties of these calculations, the molecule can be considered quasilinear. The calculated equilibrium bond angle

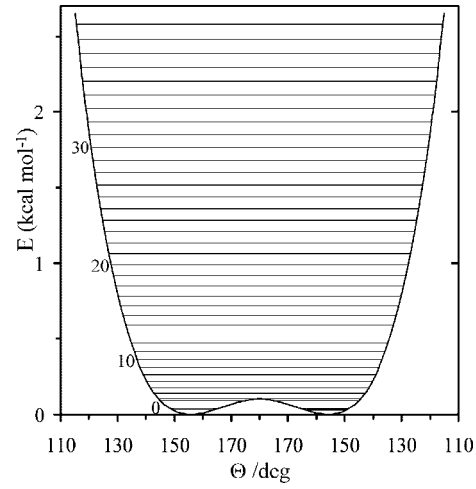

FIGURE 1. Anharmonic bending potential of $SrCl_2$ (from ref 18, Copyright 2006 Wiley-VCH, reproduced with permission).

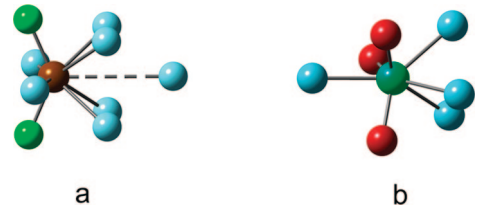

FIGURE 2. Models of molecular complexes between metal halides and matrix hosts: (a) $SrCl_2 \cdot Ar_7$, (b) $DyBr_3 \cdot Kr_4$.

is 153.5(2.5)°; yielding 144.9° after adjustments for anharmonicity and temperature, consistent with the ED bond angle, 142(4)°.

There is disagreement between the computed and experimental vibrational frequencies, determined in Ar matrix. In order to find its source, we tested the possibility of interaction between strontium and argon by simulating the matrix environment and computed the structures and vibrational frequencies of $SrCl_2 \cdot Ar_n$ ($n = 1-7$) complexes. The resulting shifts of $SrCl_2$ frequencies improved the agreement between the experimental and computed data. The strong Lewis acid character of $SrCl_2$ and the large polarizability of strontium support the possibility of host−guest interactions, and the argon atoms are strongly coordinated to the metal inducing changes in the $SrCl_2$ molecule with stabilization energies of up to about −13 kcal/mol (Figure 2a).

This type of host−guest interaction might lead to disagreements between experiments and computations when different methods yield different molecular symmetries. Lanthanide trihalides are typical examples; as the recent study of $DyBr_3$ indicates. Although most methods determined the molecule to be planar, its symmetric-stretching frequency appeared in the MI-Raman spectrum, suggesting a pyramidal geometry.[28] However, the stability of the calculated $DyBr_3 \cdot Kr_n$ complexes (Figure 2b, stabilization energy −12 kcal/mol) and the agree-

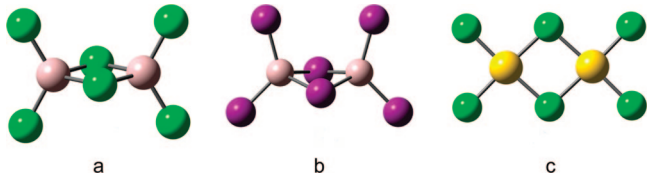

FIGURE 3. Structures of metal trihalide dimers.

ment of their frequencies with the MI-Raman data suggest complex formation in the matrix, resulting in pyramidalization of the $DyBr_3$ unit.

3.2. Floppy Oligomers and Mixed Complexes. The dimers of metal halides are always floppy, with puckering frequencies as low or lower than 20 cm^{-1}, except for the fluorides. These computed frequencies are strongly method/basis-set-dependent; therefore, the computed geometries may or may not be the real ground-state structures.

Metal trihalide dimers usually have D_{2h} symmetry, with two distorted tetrahedra sharing an edge (Figure 3a). The dimers of group 13 and group 3 trihalides have such a structure,[5,13] with some molecules apparently dissenting.[17] The DFT method yields the D_{2h} structure for Al_2I_6 as well; however, correlated calculations find the central four-member ring to be puckered (Figure 3b) and the D_{2h} structure to be a saddle point, albeit with miniscule energy difference between them, 0.2 and 0.02 kcal/mol at the MP2 and CCSD(T) levels, respectively. The results about molecular symmetry are invariant to the basis sets but are method-dependent. Gas-phase vibrational spectroscopy determined D_{2h} symmetry for Al_2I_6. In this case, the computational results may not be reliable because of the insensitivity of the computations to such small frequencies.[17]

Gold trihalide dimers also have D_{2h} symmetry but with planar geometry (Figure 3c), the reason being the participation of the 5d orbitals in the bonding and the nonparticipation of the 6p orbitals, due to relativistic effects.[7,8,10]

There has been general consensus about the halogen-bridged D_{2h} structure of metal dihalide dimers. Most linear metal dihalides have this structure, according to both computations and ED experiments (see Figure 4a).[3] However, it came as a surprise that the bent alkaline earth dihalides have different ground-state geometries, with three halogen bridges, as shown in Figure 4b.[6,27] Because only the bent monomers form C_{3v}-symmetry dimers, this could be rationalized by invoking core-polarization effects and the availability of d orbitals for bonding in the larger and soft metal dihalides.

Among the group 12 dihalide dimers, the Zn_2X_4 and Cd_2X_4 molecules have the expected D_{2h}-symmetry structure, while the Hg_2X_4 molecules have a C_{2h}-symmetry, loosely bound arrangement (Figure 4c) with little stability as a result of relativistic effects. The HgX_2 molecules are exceptionally rigid; they resist both stretching and bending due to large relativistic contraction of their s orbitals.[29]

Group 14 dihalides have also been assumed to have D_{2h}-symmetry geometry, even though this might have been suspect, considering the stereochemical activity of the lone electron pair that bends their monomers. Our calculations of the tin dihalide dimers showed that they have a C_s-symmetry ground-state structure with another one of C_{2v} symmetry somewhat higher in energy, 2.1, ~2, and 1.1 kcal/mol for the chloride, bromide, and iodide, respectively (Figure 4d,e).[12,14,21]

Stable mixed complexes of lanthanide trihalides with alkali halides are formed during the operation of metal halide discharge lamps. These complexes are typical floppy molecules, in which the connection of the alkali atom with the bridging bromine atoms is weak and dynamic. While at 0 K the tridentate form is the minimum-energy isomer, high temperatures favor the bidentate form for most complexes due to their entropy difference (Figure 5).[19]

Metal monohalides usually have complex vapor composition;[3] CuCl is an example. We carried out two ED experiments and, aided by computations, assigned the structures of dimers, trimers, and tetramers.[11] The computations found the D_{4h}-symmetry ring structure of Cu_4Cl_4 to be the ground-state structure, with another T_d-symmetry structure about 18 kcal/mol

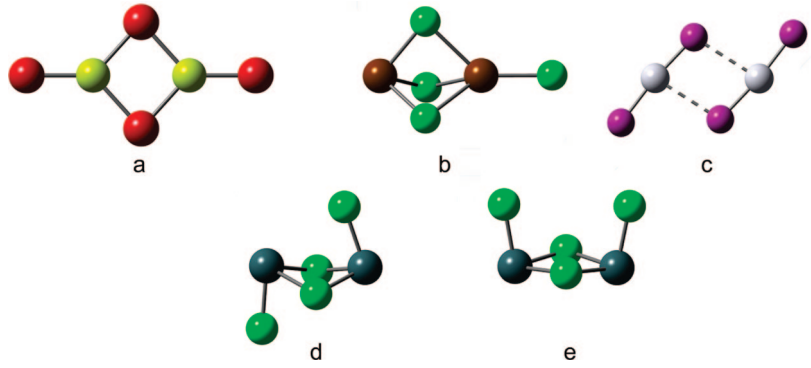

FIGURE 4. Metal dihalide dimer structures.

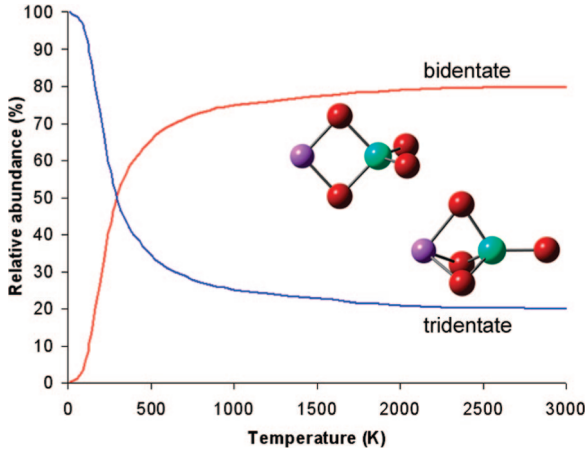

FIGURE 5. Vapor composition of mixed complexes, $AlkDyX_4$.

higher in energy, in agreement with ED. A later computation, using the same method/Cu-ECP/CI-basis set combination, except for a larger basis set on Cu, found the D_{4h} structure to be about 0.2 kcal/mol higher in energy than the D_{2d} ground state, the latter having a puckered eight-membered ring.[30] Here, ED cannot help, since the thermal-average structure that we determined was such a puckered structure in the first place, only interpreted as the result of perpendicular vibrations of a planar structure based on the computations. The question is still open whether the increasing quality of the bases and methods leads to less symmetrical structures and, if so, whether they are real and why.

Among the metal monohalide dimers, the Au_2X_2 gold halides are stabilized by strong metallophilic interactions and their dimerization is exothermic, becoming more favorable toward the iodides ($E_{dim} = -24.4$, -29.7, -33.1, and -38.3 kcal/mol for AuF, AuCl, AuBr, and AuI, respectively, at the CCSD(T) level).[10]

4. Relativistic Effects

The importance of relativistic effects on molecular structure has been recognized long ago.[31] The most obvious structural effect is the unexpected bond shortening for larger metals compared with the metals above them in the periodic table. At the nonrelativistic level, both gold and mercury halides have about 0.08 Å longer bonds than the corresponding silver and cadmium halides. On the other hand, at the relativistic level all gold monohalide bonds are about 0.05−0.06 Å *shorter* than the bonds in the corresponding silver monohalides. For the dihalides of cadmium and mercury, the relativistic bond lengths are about the same. Our calculations also show that the relativistic shortening is about 3 times larger in the sixth-row metal halides than in the fifth-row ones.[32]

Gold and mercury and their compounds are the best examples of the consequences of relativistic effects. Remarkably, their dimers, Au_2X_2 and Hg_2X_4, are very different. Unlike gold monohalides, mercury dihalides resist dimerization and form loosely bound systems with their dimerization energy decreasing toward the iodides ($E_{dim} = -6.5$ and -0.7 kcal/mol for HgF_2 and HgI_2, respectively).[29] While the magnitude of E_{dim} increases about 60% from AuF to AuI, E_{dim} of HgI_2 is a mere tenth that of HgF_2. How do we explain this very different behavior? The metallophilic interaction that stabilizes Au_2X_2 is especially strong with soft ligands, causing increasing stabilization toward the iodides. The decreasing Au···Au distance indicates this (2.809, 2.717, 2.708, and 2.722 Å, respectively, from AuF to AuI; for Au_2I_2, the very small, about 60°, Au−I−Au bond angle prevents further shortening of the Au···Au distance).[10] This interaction, however, is less likely to play a role between the mercury atoms due to their increased positive charge (q_M on Au changes from 0.65*e* to 0.41*e* in Au_2X_2 from F to I, while the same for Hg_2X_4 changes from 1.36*e* to 0.88*e*). In the absence of metallophilic interaction, the dimerization in HgX_2 is directed by electrostatic forces, and this explains why the Hg_2F_4 dimer is the most stable among the mercury dihalide dimers.

Relativistic effects explain the different behavior of gold monohalides and trihalides as well. The stability of the monohalides increases toward the larger halides, while the opposite is true for the trihalides, for which the participation of the relativistically destabilized 5d orbitals in the bonding partially compensates the effect of 6s orbital contraction.[10]

Relativistic effects are the reason for the dissimilarity between the dihalides of mercury and the other two members of group 12. They are responsible for the larger electronegativity of Hg compared with Zn and Cd and for the participation of the filled $(n - 1)$d orbitals in their bonding. The peculiar structure of the Hg_2X_4 dimers (vide supra) and the crystal structure of mercury halides, so vastly different from the rest of the group with their molecular type, is also a consequence of relativistic effects.[29]

For lanthanide trihalides, spin−orbit coupling might also be important beside scalar relativistic effects that are usually accounted for in the published ECPs. We looked into the possible effect of spin−orbit coupling in $DyCl_3$ and found that the energy lowering caused by it is small and has no effect on the geometries.[22] There is consensus that the 4f electrons do not participate in the bonding of lanthanide trihalides, although lately there have been results to the contrary.[33] For $DyCl_3$, we have found that although the f electron configuration does not change the geometry of the monomers, it makes a difference

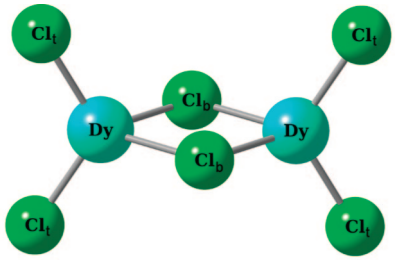

Electronic state	ΔE	Cl_t-Dy-Cl_t	Cl_b-Dy-Cl_b
	(kcal/mol)	(deg)	(deg)
$^{11}B_{2g}$, $^{11}B_{1u}$, $^{1}A_g$, $^{1}B_{2g}$, $^{1}B_{1u}$	0.0	120.1	82.5
$^{11}B_{3g}$, $^{11}A_u$,(2x)$^{11}B_{3u}$, $^{1}B_{3g}$, $^{1}A_u$	1.5	115.9	81.8
$^{11}B_{1g}$, $^{11}B_{2u}$, $^{1}B_{1g}$, $^{1}B_{2u}$	4.0	118.5	82.2

FIGURE 6. Bond angles of the Dy_2Cl_6 molecule in different electronic states.[22]

in the dimer geometries: the bond angles of the dimer in their different electronic states are consistently different as shown in Figure 6, indicating the effect of different orbital occupations.[22] The energy of the high-spin undecuplet and low-spin singlet electronic states of the dimer are nearly identical, suggesting antiferromagnetic behavior in the singlet.

5. Vibronic Interactions

5.1. Jahn–Teller Effect (JTE). The once esoteric JTE has developed into something of major importance. Its consideration has stimulated considerable structural work in the solid state (see, for example, the discovery of high-temperature superconducting ceramic materials). However, for free molecules, its observation is often difficult due to the dynamic nature of the effect. We have been fortunate in finding strong static JT distortion in free metal trihalides by ED and computations. According to CASSCF calculations, the ground-state MnF_3 molecules have a T-shaped structure with a Y-shaped structure as transition state (Figure 7 and Table 1).[4] The ED radial distribution curves (Figure 8) show that the D_{3h}-symmetry structure distorts to a lower C_{2v} symmetry (Figure 7a) as the peak corresponding to the F···F nonbonded distances splits.

The JTE describes the coupling of the electronic and vibrational motions of the molecule, causing the breakdown of the

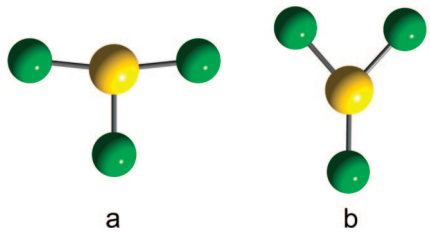

FIGURE 7. Shapes of Jahn–Teller-distorted MnF_3, AuF_3, $AuCl_3$, and AgF_3 molecules: (a) ground state; (b) transition state.

TABLE 1. Geometrical Parameters (Bond Lengths in Å, Angles in deg) and Energy Differences (kcal/mol) of Jahn–Teller Distorted Ground-State and Transition-State MX_3 Molecules from Electron Diffraction and Computation

MX_3	elec. state	ΔE	M–X1[a]	M–X2,3	X1–M–X2	method	ref
MnF_3			1.728(14)	1.754(8)	106.4(0.9)	ED, r_g, $\angle_\alpha$	4
	$^5A_1$	0.0	1.726	1.752	105.7	MP2	4
	$^5B_2$	2.1	1.773	1.731	129.1	MP2	4
AuF_3			1.893(12)	1.913(8)	102.5(1.9)	ED, r_g, $\angle_\alpha$	7
	$^1A_1$	0.0	1.902	1.911	94.4	CCSD(T)	10
	$^1A_1$	5.7	1.916	1.903	139.6	CCSD(T)	10

[a] For numbering of atoms, see Figure 9.

Born–Oppenheimer approximation. Due to its simplicity and the strong JTE observed in it, MnF_3 is an ideal example to illustrate JT coupling. The electronic configuration of the molecule in its undistorted D_{3h}-symmetry $^5E'$ state is $\sigma^1\pi^2\delta^1$. Depending on which of the doubly degenerate δ-orbitals (d_{xy} or $d_{x^2-y^2}$) will be occupied by the single electron, two different structures with different angular distortions can be envisioned as indicated in Figure 9. If the electron is on the d_{xy}-symmetry orbital, the repulsion between the charge densities of this orbital and the fluorine ligands will open one of the bond angles and lead to a T-shaped structure (C_{2v} symmetry, the d_{xy} orbital will have b_2 symmetry, giving an A_1-symmetry electronic state). By similar reasoning, the occupancy of the $d_{x^2-y^2}$ orbital (a_1 in C_{2v}) will decrease one of the bond angles and lead to a Y-shape structure with B_2 symmetry.

Gold[7,8,10] and silver trihalides[16] exhibit even stronger JTEs. For AuF_3, our ED experiments[7] agreed with the JT-distorted

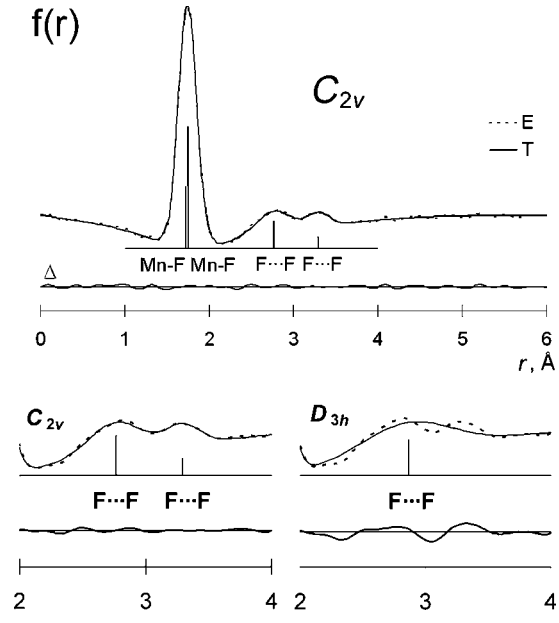

FIGURE 8. MnF_3 radial distribution function from ED: E = experimental and T = calculated for C_{2v} and D_{3h} symmetry models, respectively. The magnified F···F distance contributions indicate the difference between the C_{2v} and D_{3h} structures (from ref 4).

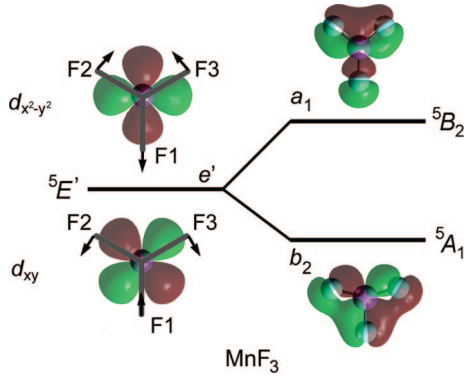

FIGURE 9. Coupling of the electronic and nuclear motions in MnF_3 leading to a T-shaped ground-state and Y-shaped transition-state structure.

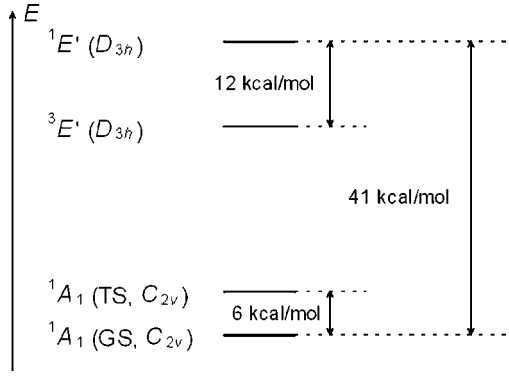

FIGURE 10. Relative energies (arbitrary scale) of different electronic states of $AuCl_3$ at the CASSCF(4,6) level. Note that the actual energies may considerably change at higher computational levels (from ref 8, Copyright 2001 American Chemical Society).

T-shaped structure for the monomer (Table 1). The transition state has a Y-shaped structure (see Figure 7b) in all these molecules. There is an important difference though between the electronic configurations of MnF_3 (d^4) and the group 11 trihalides (all d^8). According to Hund's rule, the high-spin $^3E'$ electronic state is expected to be the ground state of group 11 trihalides, and for that JTE cannot be expected because there would not be an energy gain from the distortion (two parallel-spin electrons, one on each of the two δ-orbitals). However, for the singlet $^1E'$ state, in which an electron pair occupies one of the doubly degenerate δ orbitals, strong JTE can be expected. We calculated the energies of the different electronic states of $AuCl_3$ (Figure 10);[8] apparently, the stabilization of the JT-distorted structure originating from the $^1E'$ state is so large that it "can pay the price" for the spin pairing of the otherwise lower-energy $^3E'$ state. We might call this a "JT-induced spin crossover" after Bersuker.[34]

It is of interest to follow the change in the PES of gold trihalides with the variation of the halogen (Figure 11).[10] These are so-called Mexican-hat-type PESs with the undistorted high-energy D_{3h}-symmetry structure at the center. The ground-state (minima) and the transition-state (humps) structures are located around the brim of the hat. AuF_3 has the most stable structure, with the JT stabilization energy decreasing toward the iodides. For $AuBr_3$ and AuI_3, the minimum-energy structure is not on the JT surface (vide infra). The PESs of the silver trihalides are very similar, except that these molecules are less stable than the gold trihalides and only AgF_3 is a true trihalide (vide infra).[16]

5.2. Renner–Teller Effect (RTE). RTE occurs in linear molecules that are not subject to JTE because of symmetry reasons. Due to the symmetry mismatch between the high-symmetry electronic state and the normal vibrations, the linear vibronic coupling terms are zero. However, there can still be considerable quadratic terms in the vibronic coupling and if this happens, distortions might occur.[35] This is the RTE.

Chromium dihalides are emblematic examples of JTE in crystals; their octahedral configuration undergoes tetragonal distortion leading to a D_{4h}-symmetry arrangement. The JTE does not apply to their gas-phase molecules, and they have been expected to be linear. A computation, however, sug-

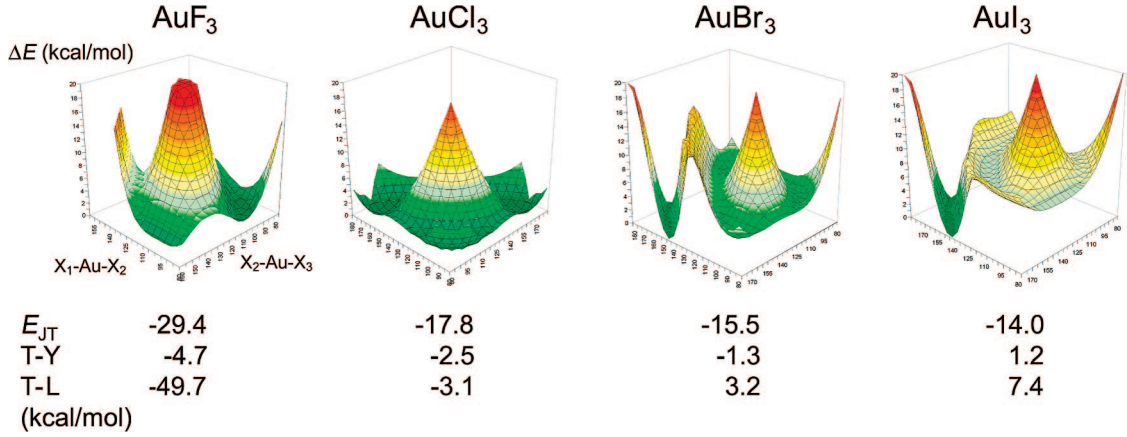

FIGURE 11. Potential energy surfaces (B3LYP) of gold trihalides. E_{JT} = JT stabilization energy; T = ground state; Y = transition state; L = $AuX \cdot X_2$ molecule representing the minimum structures of $AuBr_3$ and AuI_3 (from ref 10, Copyright 2001 Wiley-VCH, by permission).

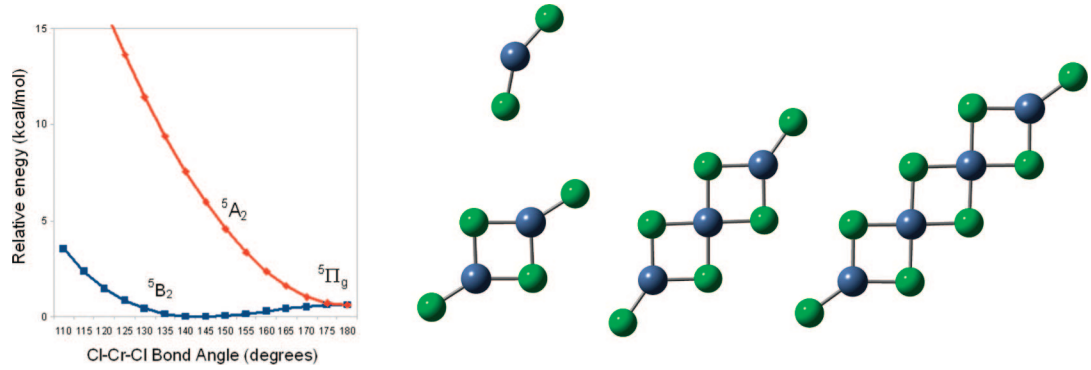

FIGURE 12. (a) Renner–Teller bending potential of $CrCl_2$ and (b) structures of the monomer and oligomers (from ref 23, Copyright 2008 Wiley-VCH, by permission).

gested $CrCl_2$ to be bent in its ground electronic state, due to RTE,[36] and our combined ED and computational study confirmed this (Figure 12a).[23] The ED bond angle is 149(10)°, in agreement with the computations (between 143° and 167° depending on the method; the shallow bending potential makes the determination of the bond angle difficult) and is indicative of the RTE. The estimated equilibrium Cr–Cl bond length from electron diffraction, 2.196(20) Å, beautifully agrees with the CCSD(T) value of 2.194 Å.[23]

Chromium dichloride is unique among transition metal dihalides in having a complex vapor composition with oligomers up to perhaps tetramers. The dimer has a four-membered halogen-bridged structure being repeated in the lowest-energy structures of oligomers (Figure 12b). They directly lead to the crystal of α-$CrCl_2$ consisting of antiferromagnetically coupled Cr_2Cl_2 units. Similarly, the global-minima structures of all clusters are antiferromagnetically coupled. Thus, nucleation starts early on in $CrCl_2$, with the four-membered chain motif. The ED data confirmed the chain structure of the trimer, while the usual six-membered ring trimer model did not fit the experimental data.[23]

6. Molecules in the Computer

Computations often result in unexpected molecular geometries differing from assumed stereotypes. Systematic studies of groups of substances may yield heretofore unknown structures that appear to be thermodynamically stable. There is natural excitement over such discoveries, but Hoffmann, Schleyer, and Schaefer recently called for caution in declaring a molecule "stable".[37] Nonetheless, a few such molecules from our work will be briefly mentioned here.

Our study of gold[10] and silver[16] trihalides led to unexpected L-shaped minimum-energy geometries (Figure 13). This structure was found to be the minimum for $AuBr_3$ (Figure 11), with a high barrier (8 kcal/mol) from the JT PES. However, for gold triiodide, the energy barrier is merely 2 kcal/mol. It might be possible to observe this molecule in an experiment because the reaction $AuI + I_2 \rightarrow AuI \cdot I_2$ is exothermic (−22 kcal/mol) and the formation of the L-shaped molecule happens without an activation barrier. Once this molecule is formed, it should be stable because the activation barrier toward AuI_3 is about 8 kcal/mol. In the L-shaped molecule one of the triiodide bonds disappears (here M–I3); instead, there is a new I–I bond. This molecule is a typical donor–acceptor complex, in which I_2 acts as donor and AuI as acceptor (the LUMO of AuX is an antibonding σ_g^* molecular orbital, while the HOMO of X_2 is an antibonding π_g MO). Among the silver trihalides, the global minimum is this L-shaped structure for all, except AgF_3. Thus, in the three heavier silver trihalides, silver does not appear in the usual oxidation state, 3.

We have computed the structures of silver subhalides, Ag_2X.[16] Their ground-state structure has C_{2v} symmetry and the molecules can be best described as $[Ag_2]^+X^-$, with a covalently bonded Ag_2^+ ion in Coulombic interaction with the halide ions. The spin densities show that the odd electron density is localized on the Ag_2 unit, between the two Ag centers (Figure 14); and the Wiberg index is close to that in the free ion. All four silver subhalides appear thermodynamically stable; thus, they might be prepared unless prevented by kinetic barriers. While all silver monohalides are common, of the other valencies of silver, only the fluorides are known, Ag_2F, AgF_2, and AgF_3. Our calculations showed the other silver tri-

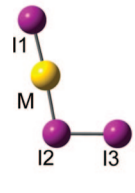

		Ag	Au
$MI \cdot I_2$, (Å)	M–I1	2.562	2.593
	M–I2	2.722	2.684
	M··I3	4.330	4.221
	I2–I3	2.576	2.779
$MI \cdot I_2 \rightarrow MI + I_2$, (kcal/mol)		19	23
MI, (Å)		2.551	2.590
I_2, (Å)		2.688	2.760

FIGURE 13. Ground-state geometries of gold and silver triiodides.[10,16]

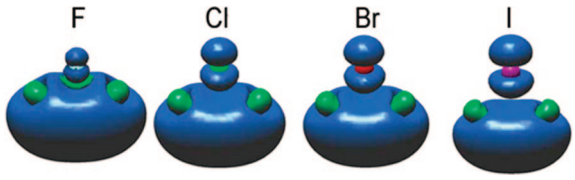

FIGURE 14. Spin densities of the ground-state Ag_2X molecules (HF densities at the CCSD(T) geometries, from ref 16, Copyright 2005 American Chemical Society).

halides to be stable in their L-shaped, $AgX \cdot X_2$ ground electronic states; whereas of the dihalides, only AgF_2 seems to be stable.

7. Conclusion and Outlook

Combined application of state-of-the-art experimental and computational techniques moved the structural chemistry of metal halides to a new level, where we can probe into their bonding peculiarities further than it had ever been possible. Due to the rapid advances in the computational share in these studies, it is increasingly important to realize the differences in the physical meaning of the structural information originating from different techniques.

We have shown that many metal halides have lower-symmetry structures than had been assumed. Some of these geometries are the result of strong vibronic interactions—Jahn–Teller, Renner–Teller, or pseudo-Jahn–Teller effects—that bring about profound structural changes in the halides of certain metals with partially filled orbitals. Other variations might be the result of the stereochemical activity of a lone electron pair. New computations often result in lower-symmetry structures for dimers and oligomers of metal halides with too-low-frequency vibrations, and these structures have to be looked upon with caution because they might be spurious, caused by the insensitivity of computations.

Our studies have provided further evidence that relativistic effects have profound structural consequences, as the examples of gold and mercury halides indicate. These appear as bond shortenings, unusual molecular symmetries, and unusual structure preferences in the crystal. The increasing potentials of computations bring about new heretofore unknown and intriguing structures that might or might not be feasible, but are exciting nonetheless.

Because computations of metal halides are costly and time-consuming, a comment is appropriate. The level of computation should be chosen depending on its goal; if it is thermodynamic properties for industrial applications, relatively small basis sets, such as triple-ζ, with large-core ECPs and density functional calculations suffice. However, if our goal is the understanding of fine structural details, very large basis sets and high-level wave function-based correlated calculations are needed.

Looking at the progress of computational chemistry, we anticipate an increasing role for computations in molecular structure studies in general and of metal halides in particular. This progress will shed light on more and more intricate details of molecular structures, thus deepening our understanding of their governing principles. We can also expect increasing interest in research on the boundaries of different states of matter; including not only gas-phase molecules and their crystals but also the most difficult in-between states, melts and solutions. Slight steps have already been taken in this area, starting with studying the transition between gas-phase and crystal-phase structures.[27,29,38]

The day this Conclusion was written, the much-debated Large Hadron Collider at CERN became operational. There are enormous expectations toward what it might uncover, and we still have to wait and see what happens. But it already demonstrates the ever increasing potentials of and expectations toward science and toward humanity's desire to know more about the yet unknown, whether it is on atomic, molecular, or cosmic scale.

My studies of metal halides could not have been carried out without the work of my students and the constructive and enjoyable collaboration with many of my colleagues all over the world; I thank them all. Special thanks go to Mr. Zoltán Varga for his invaluable help in the preparation of drawings. I appreciate the helpful suggestions of one of the referees. I also acknowledge the Hungarian National Research Funds (Grant OTKA K 60365) for supporting our research.

Note Added in Proof. After the submission of this Account, we have completed and published a joint computational and ED study of CrF_2, whose ground electronic state was found to be a Renner–Teller distorted quasi-linear $^5B_2$ state by computation. At the high temperature conditions of the ED experiment molecules of three different electronic states were present (Vest, B.; Schwerdtfeger, P.; Kolonits, M.; Hargittai, M. Chromium difluoride: Probing the limits of structure determination. *Chem. Phys. Lett.*, **2009**, *468*, 143–147).

BIOGRAPHICAL INFORMATION

Magdolna Hargittai received her Ph.D. (1978), and D.Sc. degrees (1991) from the Hungarian Academy of Sciences (HAS) in Budapest. She is Member of the HAS (2004) and of the Academia Europaea (2006). She is Research Professor at the Materials Structure and Modeling Research Group of the HAS at the

Budapest University of Technology and Economics. Besides her research publications, she has coauthored 8 and edited 11 books; among them *Symmetry through the Eyes of a Chemist* (third edition, 2009), *Visual Symmetry* (2009), and the *Candid Science* series.

REFERENCES

1 Hargittai, M. The molecular geometry of gas-phase metal-halides. *Coord. Chem. Rev.* **1988**, *91*, 35–88.

2 Hargittai, M. In *Stereochemical Applications of Gas-Phase Electron Diffraction. Part B*; Hargittai, I., Hargittai, M., Eds.; VCH Publishers: New York, 1988; pp 383−454.

3 Hargittai, M. Molecular structure of metal halides. *Chem. Rev.* **2000**, *100*, 2233–2301.

4 Hargittai, M.; Réffy, B.; Kolonits, M.; Marsden, C. J.; Heully, J. L. The structure of the free MnF_3 molecule—A beautiful example of the Jahn−Teller effect. *J. Am. Chem. Soc.* **1997**, *119*, 9042–9048.

5 Réffy, B.; Kolonits, M.; Hargittai, M. Gallium tribromide: Molecular geometry of monomer and dimer from gas-phase electron diffraction. *J. Mol. Struct.* **1998**, *445*, 139–148.

6 Levy, J. B.; Hargittai, M. Unusual dimer structures of the heavier alkaline earth dihalides: A density functional study. *J. Phys. Chem. A* **2000**, *104*, 1950–1958.

7 Réffy, B.; Kolonits, M.; Schulz, A.; Klapötke, T. M.; Hargittai, M. Intriguing gold trifluoride—Molecular structure of monomers and dimers: An electron diffraction and quantum chemical study. *J. Am. Chem. Soc.* **2000**, *122*, 3127–3134.

8 Hargittai, M.; Schulz, A.; Réffy, B.; Kolonits, M. Molecular structure, bonding, and Jahn−Teller effect in gold chlorides: Quantum chemical study of $AuCl_3$, Au_2Cl_6, $AuCl_4^-$, AuCl, and Au_2Cl_2 and electron diffraction study of Au_2Cl_6. *J. Am. Chem. Soc.* **2001**, *123*, 1449–1458.

9 Hargittai, M.; Kolonits, M.; Schultz, G. The molecular structure of barium dibromide: An electron diffraction and quantum chemical study. *J. Mol. Struct.* **2001**, *567*, 241–246.

10 Schulz, A.; Hargittai, M. Structural variations and bonding in gold halides: A quantum chemical study of monomeric and dimeric gold monohalide and gold trihalide molecules, AuX, Au_2X_2, AuX_3, and Au_2X_6 (X = F, Cl, Br, I). *Chem.—Eur. J.* **2001**, *7*, 3657–3670.

11 Hargittai, M.; Schwerdtfeger, P.; Réffy, B.; Brown, R. The molecular structure of different species of cuprous chloride from gas-phase electron diffraction and quantum chemical calculations. *Chem.—Eur. J.* **2003**, *9*, 327–333.

12 Levy, J. B.; Jancsó, G.; Hargittai, M. Structure and thermodynamics of the tin dichloride dimer—A computational study. *J. Phys. Chem. A* **2003**, *107*, 10450–10455.

13 Réffy, B.; Marsden, C. J.; Hargittai, M. Molecular geometry of monomeric and dimeric yttrium trichloride from gas-phase electron diffraction and quantum chemical calculations. *J. Phys. Chem. A* **2003**, *107*, 1840–1849.

14 Kolonits, M.; Réffy, B.; Jancsó, G.; Hargittai, M. Molecular structure and thermochemistry of tin dibromide monomers and dimers. A computational and electron diffraction study. *J. Phys. Chem. A* **2004**, *108*, 6778–6783.

15 Hargittai, M. High-temperature gas-phase electron diffraction: Unexpected dimer structures among metal halides. *Struct. Chem.* **2005**, *16*, 33–40.

16 Müller-Rösing, H.-C.; Schulz, A.; Hargittai, M. Structure and bonding in silver halides. A quantum chemical study of the monomers: Ag_2X, AgX, AgX_2, AgX_3 (X = F, Cl, Br, I). *J. Am. Chem. Soc.* **2005**, *127*, 8133–8145.

17 Hargittai, M.; Kolonits, M.; Réffy, B. An intricate molecule: Aluminum triiodide. Molecular structure of AlI_3 and Al_2I_6 from electron diffraction and computation. *J. Phys. Chem. A* **2006**, *110*, 3770–3777.

18 Varga, Z.; Lanza, G.; Minichino, C.; Hargittai, M. Quasilinear molecule par excellence, $SrCl_2$: Structure from high-temperature gas-phase electron diffraction and quantum-chemical calculations—Computed structures of $SrCl_2$−argon complexes. *Chem.—Eur. J.* **2006**, *12*, 8345–8357.

19 Varga, Z.; Hargittai, M. The $NaDyBr_4$ complex: Its molecular structure and thermodynamic properties. *Struct. Chem.* **2006**, *17*, 225–233.

20 Hargittai, M.; Varga, Z. Molecular constants of aluminum monohalides: Caveats for computations of simple inorganic molecules. *J. Phys. Chem. A* **2007**, *111*, 6–8.

21 Neizer, Z.; Varga, Z.; Jancsó, G.; Hargittai, M. Vapor phase tin diiodide: Its structure and thermodynamics, a computational study. *Struct. Chem.* **2007**, *18*, 641–648.

22 Lanza, G.; Varga, Z.; Kolonits, M.; Hargittai, M. On the effect of 4f electrons on the structural characteristics of lanthanide trihalides. Computational and electron diffraction study of dysprosium trichloride. *J. Chem. Phys.* **2008**, *128*, 0743011−14.

23 Vest, B.; Varga, Z.; Hargittai, M.; Hermann, A.; Schwerdtfeger, P. The elusive structure of $CrCl_2$—A combined computational and gas phase electron diffraction study. *Chem.—Eur. J.* **2008**, *14*, 5130–5143.

24 Hargittai, M. Comment on "A theoretical study of bonding in lanthanide trihalides by density functional methods". *J. Phys. Chem. A* **1999**, *103*, 7552–7553.

25 Hargittai, M.; Hargittai, I. Experimental and computed bond lengths—The importance of their differences. *Int. J. Quantum Chem.* **1992**, *44*, 1057–1067.

26 Quantum Inorganic Chemistry. *Faraday Discuss.* **2003**, *124*, 1−455.

27 Donald, K. J.; Hoffmann, R. Solid memory: Structural preferences in group 2 dihalide monomers, dimers, and solids. *J. Am. Chem. Soc.* **2006**, *128*, 11236–11249.

28 Groen, C. P.; Varga, Z.; Kolonits, M.; Peterson, K. A.; Hargittai, M. Does the f electron configuration affect molecular geometries? A joint computational, vibrational spectroscopic, and electron diffraction study of dysprosium tribromide. *Inorg. Chem.*, submitted for publication.

29 Donald, K. J.; Hargittai, M.; Hoffmann, R. Group 12 dihalides. Structural predilections from gases to solids. *Chem.—Eur. J.* **2008**, *15*, 158–177.

30 Schwerdtfeger, P.; Krawczyk, R. P.; Hammerl, A.; Brown, R. A comparison of structure and stability between the group 11 halide tetramers M_4X_4 (M = Cu, Ag, or Au; X = Cl, Br, or I) and the group 11 chloride and bromide phosphanes $(XMPh_3)_4$. *Inorg. Chem.* **2004**, *43*, 6707–6716.

31 Pyykko, P. Relativistic effects in structural chemistry. *Chem. Rev.* **1988**, *88*, 563–594.

32 Varga, Z.; Hargittai, M. Manuscript in preparation, 2008.

33 Clavaguera, C.; Dognon, J. P.; Pyykko, P. Calculated lanthanide contractions for molecular trihalides and fully hydrated ions: The contributions from relativity and 4f-shell hybridization. *Chem. Phys. Lett.* **2006**, *429*, 8–12.

34 Garcia-Fernandez, P.; Bersuker, I. B.; Boggs, J. E. Orbital disproportionation and spin crossover as a pseudo Jahn-Teller effect. *J. Chem. Phys.* **2006**, *125*, 104102.

35 Bersuker, I. B. *Electronic Structure and Properties of Transition Metal Compounds*; John Wiley & Sons: New York, 1996.

36 Jensen, V. R. Chromium dichloride: The unusually flat bending potential of the (5)Pi(g)-derived B-5(2) ground state. *Mol. Phys.* **1997**, *91*, 131–137.

37 Hoffmann, R.; Schleyer, P. v. R.; Schaefer, H. F., III. Predicting molecules—More realism, please! *Angew. Chem., Int. Ed* **2008**, *47*, 7164–7167.

38 Krawczyk, R. P.; Hammerl, A.; Schwerdtfeger, P. Coinage metal halide clusters: From two-dimensional ring to three-dimensional solid-state-like structures. *ChemPhysChem* **2006**, *7*, 2286–2289.